

Diabatic Heating as a Diagnostic for Weather and Climate

David M. Straus (COLA, George Mason Univ.)

Acknowledgments:

Daniela I. V. Domeisen (Univ. of Lausanne, ETH Zurich)

Sarah-Jane Lock (ECMWF)

Franco Molteni (ECMWF)

Priyanka Yadav (ETH Zurich, NASA)

Ben Cash, Erik Swenson, Heidi Nsiah



Why Diabatic Heating?

- (1) Total Diabatic Heating is the driving engine for general circulation of the atmosphere**
- (2) Tropical Diabatic Heating drives the extra-tropical response to phenomena such as ENSO and the MJO → Implications for predictability**
- (3) Diabatic Heating in mid-latitude cyclones changes the structure of the cyclones and the configuration of the storm tracks**
- (4) Diabatic Heating is an integral part of Monsoonal Oscillations**

**Why isn't precipitation enough?
(It gives us the vertical integral of latent heating)**

- (1) Radiative Heating, Surface Sensible Heating and Diffusive Heating should be taken into account.**
- (2) The vertical structure of the Heating may be important
(but more on this later ...)**
- (3) Precip. is hard to measure, and models do not handle it well.**

Some Cautions:

- (1) Diabatic Heating can not be measured directly, although it can be inferred from satellite measurements of radiation, from radar, ...**
- (2) Diabatic Heating is (or should be) an output of models, but how to compare to observations?**
- (3) Uniform estimation of Apparent Heating as a residual in the thermodynamic budget (Yanai) is a useful technique and is used here.**

Intrinsic Predictability Limits arising from Indian Ocean MJO Heating: Effects on tropical and extratropical teleconnections

David M. Straus¹, Daniela I.V. Domeisen^{3,4}, Sarah-Jane Lock², Franco Molteni², and Priyanka Yadav⁴

¹Center for Ocean-Land-Atmosphere Studies, George Mason University, Fairfax, VA, USA

²European Centre for Medium-Range Forecasts, Reading, UK

³University of Lausanne, Lausanne, Switzerland

⁴Institute for Atmospheric and Climate Science, ETH Zurich, Zurich, Switzerland

Thanks to Prof. Barry Klinger (GMU) for plotting spectra.

Straus, D. M., Domeisen, D. I. V., Lock, S.-J., Molteni, F., and Yadav, P.: Intrinsic predictability limits arising from Indian Ocean Madden–Julian oscillation (MJO) heating: effects on tropical and extratropical teleconnections, *Weather Clim. Dynam.*, **4**, 1001–1018, <https://doi.org/10.5194/wcd-4-1001-2023>, 2023.



Intrinsic Predictability Limits of the S2S Response to the MJO

Tropical heating in general is highly intermittent in space and time

This is true even *even within a single episode of the MJO*.

The precise evolution of the heating is therefore presumably not predictable on S2S time scales.

Goal: Study the limits on predictability that are imposed by our inability to predict the precise space-time evolution of the MJO tropical heating, even if we can predict its envelope.

A Model Study (ECMWF's Integrated Forecast System – IFS Cycle 43r3)
Stochastic Parameterization (perturbations) an integral part of IFS

Ensemble reforecasts from MJO initial conditions (61-days)

For each initial condition, the ensemble members differ from each other **only because of perturbations introduced throughout the run in the tropical Indo-Pacific region. (*The initial conditions are NOT perturbed*)**

The ensemble spread is entirely due to the uncertainty in the output of the physical parameterizations in the tropical Indo-Pacific region.

Experimental Configuration

ECMWF IFS Cycle 43r3

Atmospheric Model Resolution: 36 km horiz. resolution – 91 levels up to 0.01 Pa

NEMO Ocean Model v3.4.1 (1/4 degree horiz. resolution)

INITIAL CONDITIONS (all having MJO phases 2 and 3 at initial time)

8 start dates for 1 Nov (different years), 5 start dates for 1 Jan (different years)

Reforecasts for 61 days, each with an ensemble of 51 members (so 663 reforecasts in total)

Perturbations: The ECMWF model incorporates stochastic perturbations to the tendencies produced by sub-grid scale processes *as an integral part of the model*, so the only change we have made is to limit the application of these perturbations to the tropical Indo-Pacific region

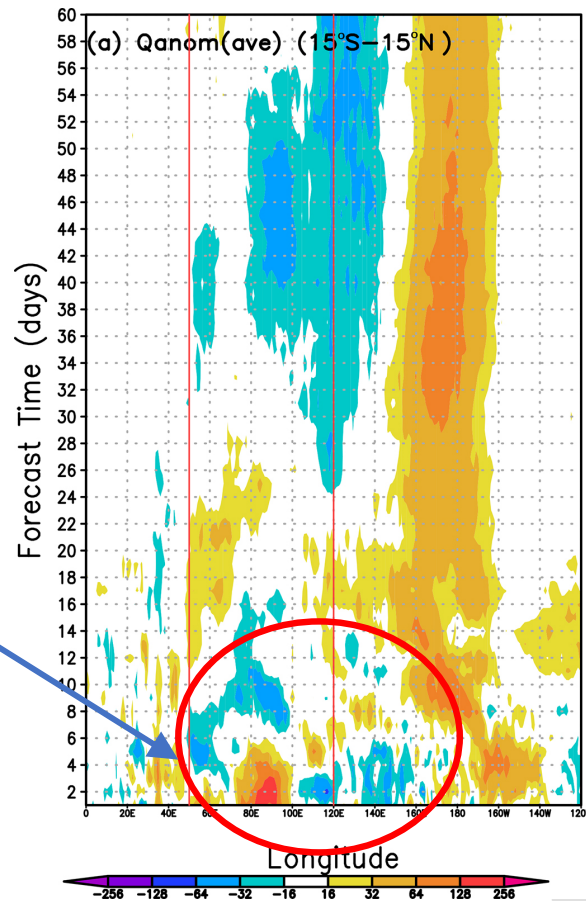
Table 1. Summary of the model runs performed for this study, for the November start dates (left) and the January start dates (right).

Start date	Ensemble size	Start date	Ensemble size
01 Nov 1986	50+1	01 Jan 1987	50+1
01 Nov 1987	50+1	01 Jan 1990	50+1
01 Nov 1990	50+1	01 Jan 1995	50+1
01 Nov 2001	50+1	01 Jan 2010	50+1
01 Nov 2002	50+1	01 Jan 2013	50+1
01 Nov 2004	50+1		
01 Nov 2011	50+1		
01 Nov 2015	50+1		
01 Nov 1981..2016	8+1	01 Jan 1981..2016	8+1

Daily Ensemble Mean
of vertically integrated
diabatic heating

Longitude Time Plot

MJO signal is apparent
in the first 10 days



Daily Ensemble Spread
of vertically integrated
diabatic heating

Longitude Time Plot

Red dotted lines give
the region of
perturbations

Note large spread
compared to signal

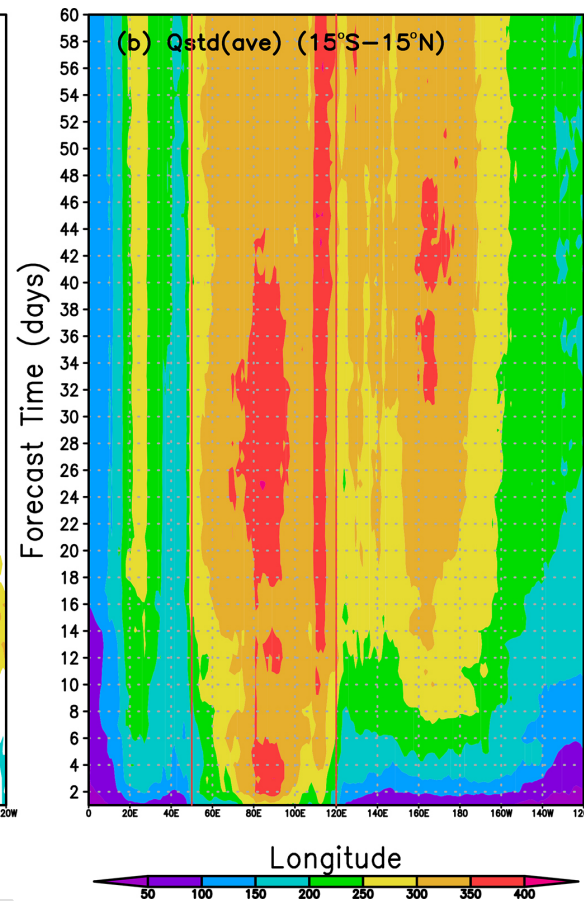
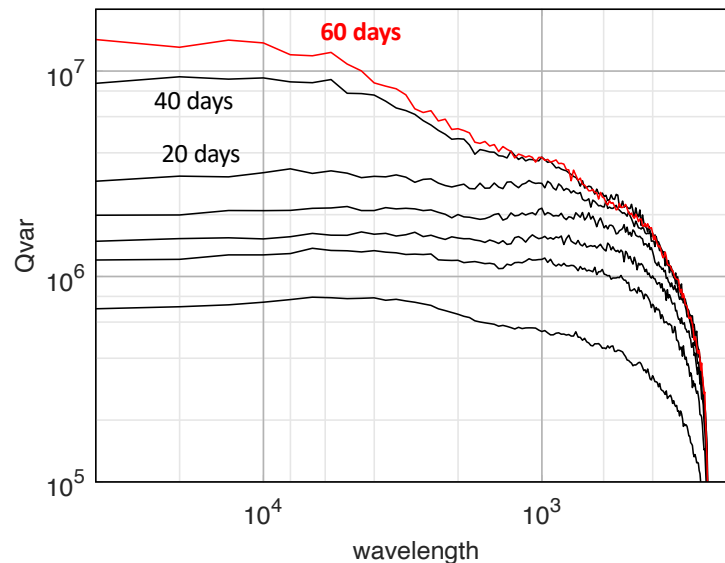


Figure 1. (a) Evolution of the daily mean, ensemble mean anomaly of diabatic heating anomaly Q (averaged 15°S – 15°N) for days 1–60 of the 60d experiments averaged over all experiments. (b) The evolution of the ensemble standard deviation of the daily mean heating (vertically integrated and averaged 15°S – 15°N) averaged over all experiments. The abscissa gives the forecast time in days. The red lines indicate the range of longitudes over which the stochastic parametrization was applied. Units are watts per square meter (W m^{-2}).

Error Spectra of Tropical Heating

- nearly white (flat spectrum) initially associated with localized heating error
- Errors at largest scales grow most slowly. Even after 40 days the largest scales have not saturated.
- some expectation that mid-latitude response most sensitive to largest scales of heating)

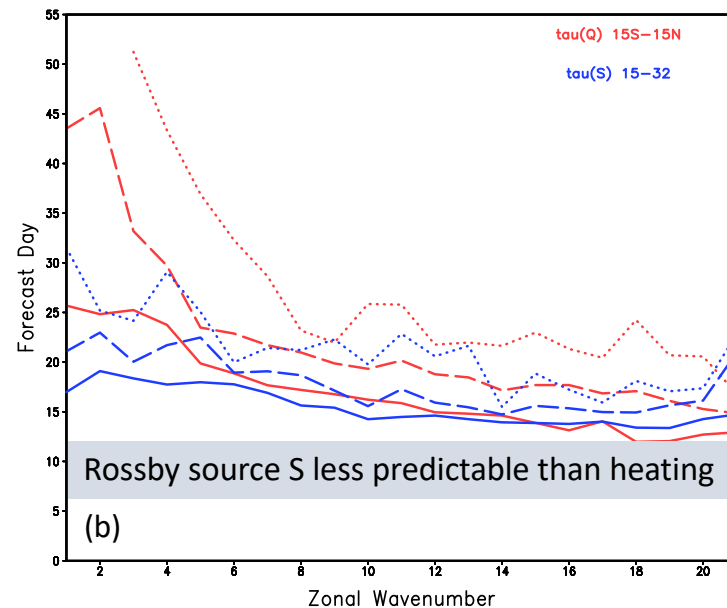
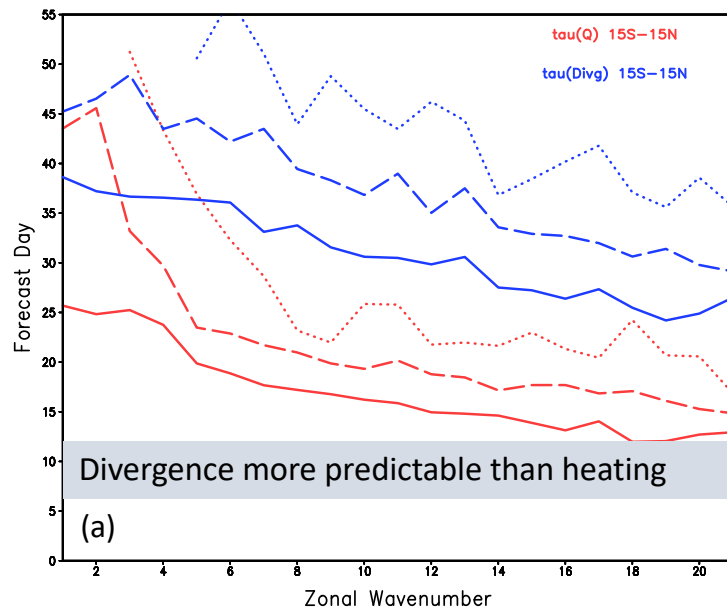


Zonal wavenumber spectra of error variance in mid-level tropical diabatic heating Q_{mid}^* (avg 15S-15N). Black lines give error of 2-day averaged Q_{mid} for 1-2 days, 3-4 days, 5-6 days, 9-10 days, 19-20 days and 39-40 days. Red line gives error for days 59-60. (Heating averaged between 850 and 400 hPa)

Predictability Times

Times (τ) at which error variance reaches a certain fraction of saturation as a function of zonal wavenumber

solid lines : error variance reaches 50% of saturation
 dashed lines: error variance reaches 70% of saturation
 dotted lines: error variance reaches 90% of saturation



Predictability Times for Heating
 Predictability Times for 200 hPa divergence
 both averaged 15S – 15N

Diabatic Heating

Predictability Times for Heating
 Predictability Times for S (Rossby Wave Source)
 Rossby Wave Source averaged 15N – 32N


David Straus ECOMS Workshop

Comparison of Predictability Times for the Largest Scales

- Although the uncertainty in heating is huge, the largest-scale component of heating is fairly predictable
- Tropical upper-level divergence is **more** predictable than heating. The divergence in some sense integrates over details of the heating
- Subtropical Rossby Wave Source is **less** predictable than the heating !!

Preferred intra-seasonal circulation patterns of the Indian summer monsoon and active-break cycles

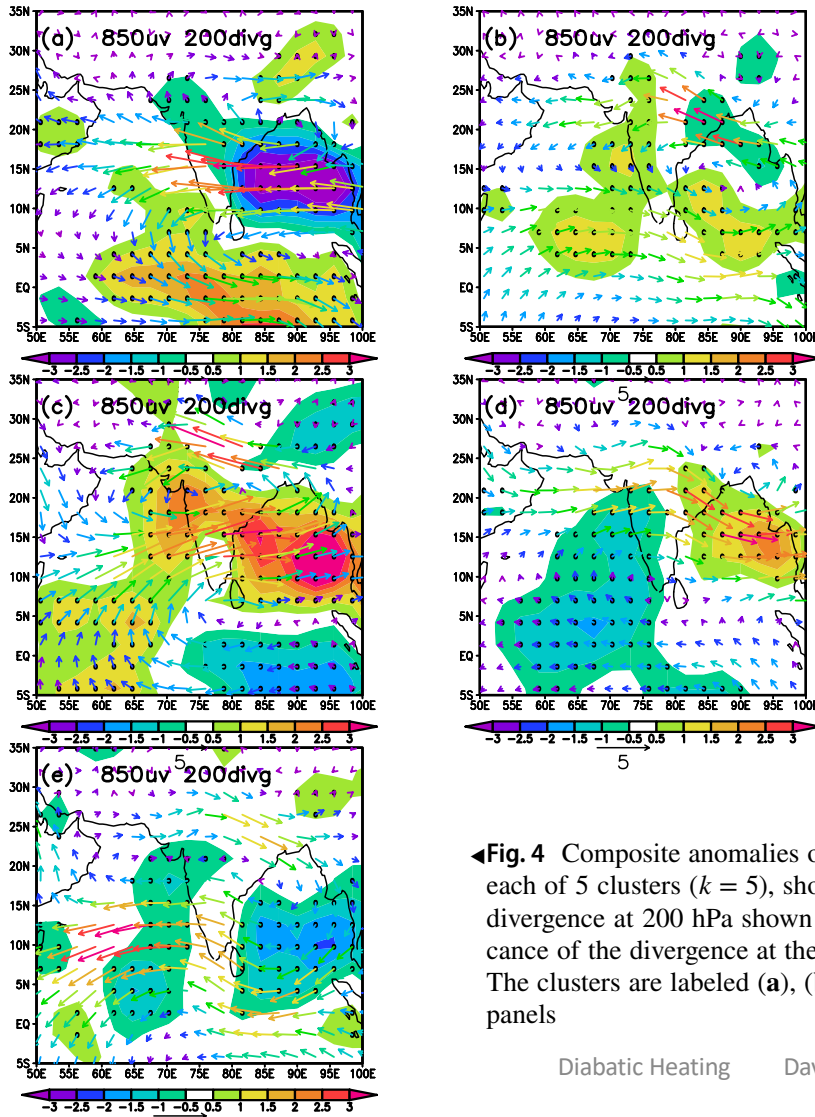
A new view of the active-break cycle

David M. Straus¹ 

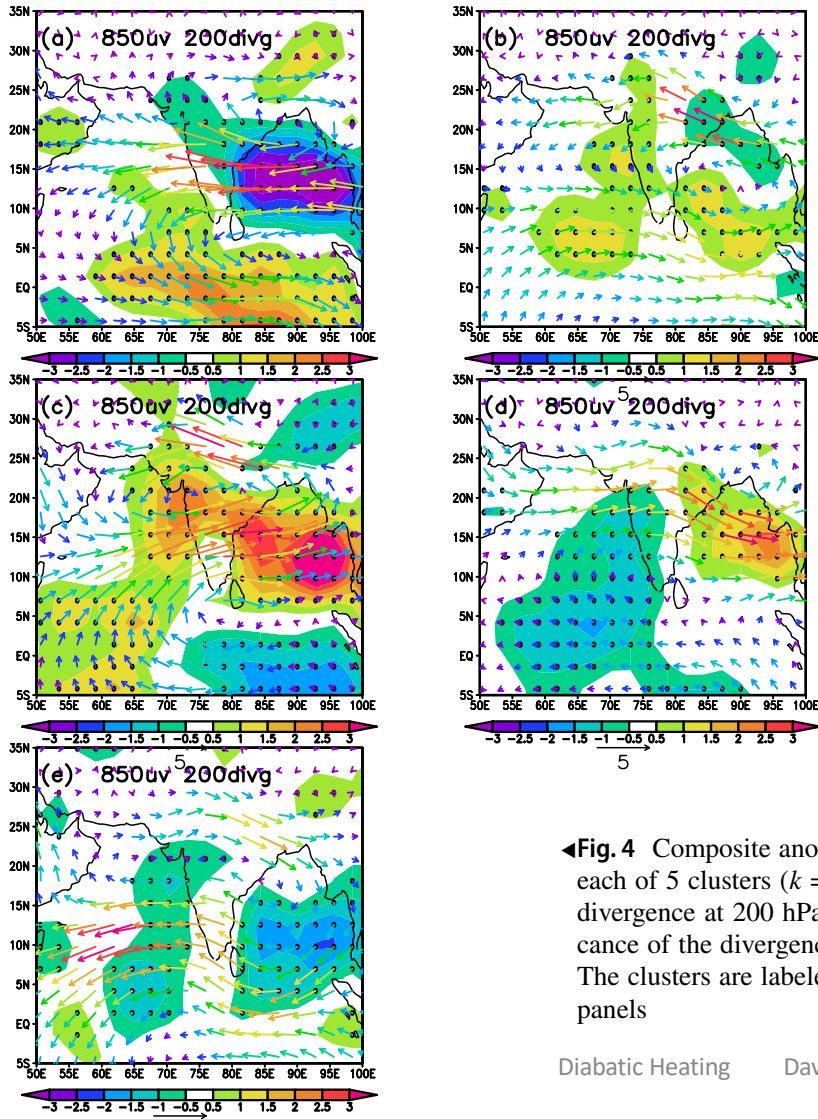
Cluster Analysis of 850 circulation (u,v) for pentads during boreal summer (Jun-Sept) from 1979-2018 (ERA-Interim)

Shown are cluster composite anomalies of (u,v) and 200 hPa divergence. Composites of obs. rainfall are similar

Looks like active-break cycle if we order the maps a certain way! (a)→(b)→(c)→(d)→(e)→(a)



◀**Fig. 4** Composite anomalies of horizontal winds (u, v) at 850 hPa for each of 5 clusters ($k = 5$), shown in vectors. Composite anomalies of divergence at 200 hPa shown in shading, in units of $10^{-6} s^{-1}$. Significance of the divergence at the 95% level is indicated by the stippling. The clusters are labeled (a), (b), (c), (d) and (e) corresponding to the panels



◀**Fig. 4** Composite anomalies of horizontal winds (u, v) at 850 hPa for each of 5 clusters ($k = 5$), shown in vectors. Composite anomalies of divergence at 200 hPa shown in shading, in units of 10^{-6}s^{-1} . Significance of the divergence at the 95% level is indicated by the stippling. The clusters are labeled (a), (b), (c), (d) and (e) corresponding to the panels

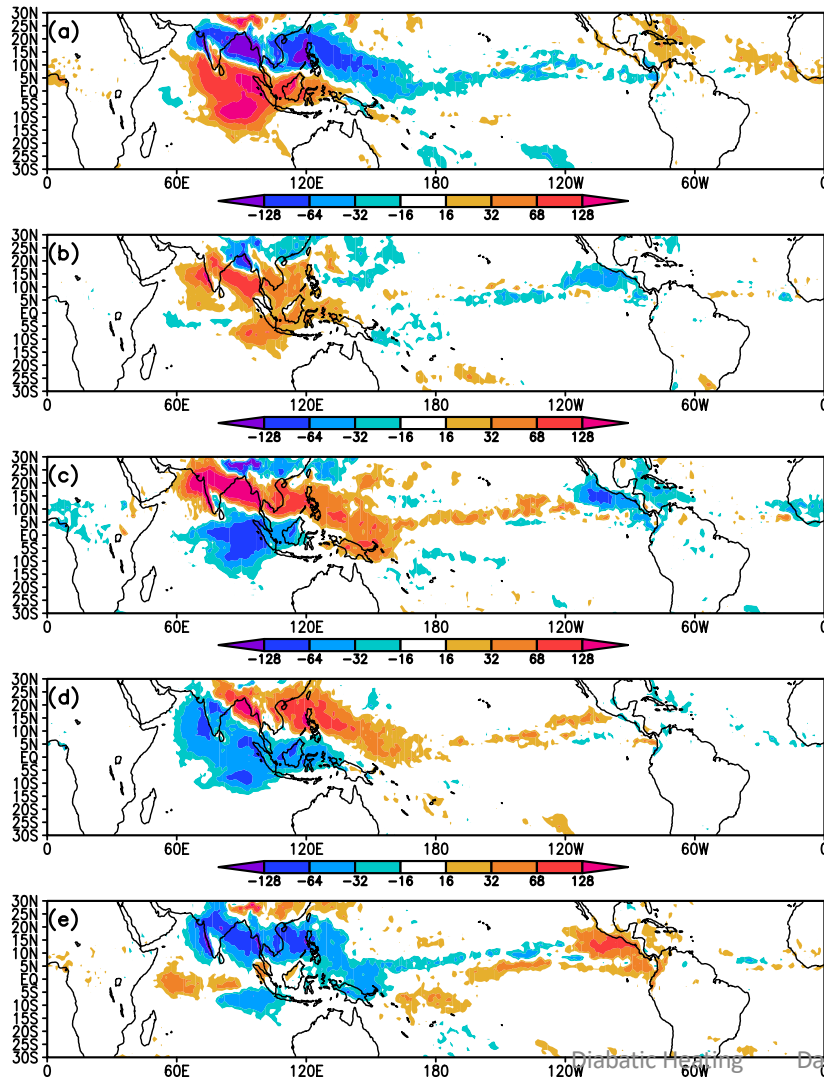
Table 5 Transition table for 5 clusters

COLUMN	(a)	(b)	(c)	(d)	(e)
ROW M					
(a)	59	45	8	12	34
(b)	30	63	47	33	23
(c)	6	18	53	54	13
(d)	19	39	23	92	48
(e)	43	31	16	36	75

Elements give number of transitions from cluster M (row) to column (N). The off-diagonal elements significant at the 95% confidence level are given in bold font

Looks like active-break cycle if we order the maps a certain way! (a)→(b)->(c)->(d)->(e)->(a)

This is confirmed by transitions that are significantly different from random!



◀ **Fig. 8** Composite anomalies of vertically integrated diabatic heating for each of 5 clusters ($k = 5$), in units of $W m^{-2}$. The color scale applies to all panels. The clusters are labeled (a), (b), (c), (d) and (e) corresponding to the panels

Preferred cycle:
 (a)→(b)->(c)->(d)->(e)->(a)

Tropics-Wide composites of vertically integrated diabatic heating in $W m^{-2}$ shows the canonical Boreal Summer Intra-Seasonal Oscillation (BSISO).

Heating gives a unified picture

How do changes in model parameterization(s) affect diabatic heating?

Example of a Recent ECMWF model change:

From: SPPT (tendencies resulting of parameterized physics schemes are perturbed)

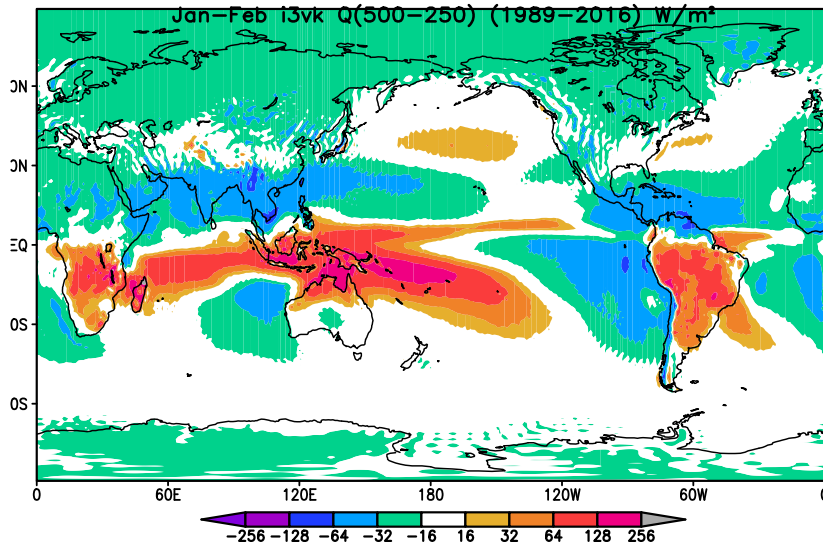
To: SPP (physical parameters within the schemes are randomly perturbed)

Forecasts of Jan-Feb for 28 years (initialized 01 Jan: 1989-2016): 9 ensemble members
CY48R1.0 at resolution TCo319L137 / ORCA025Z_75

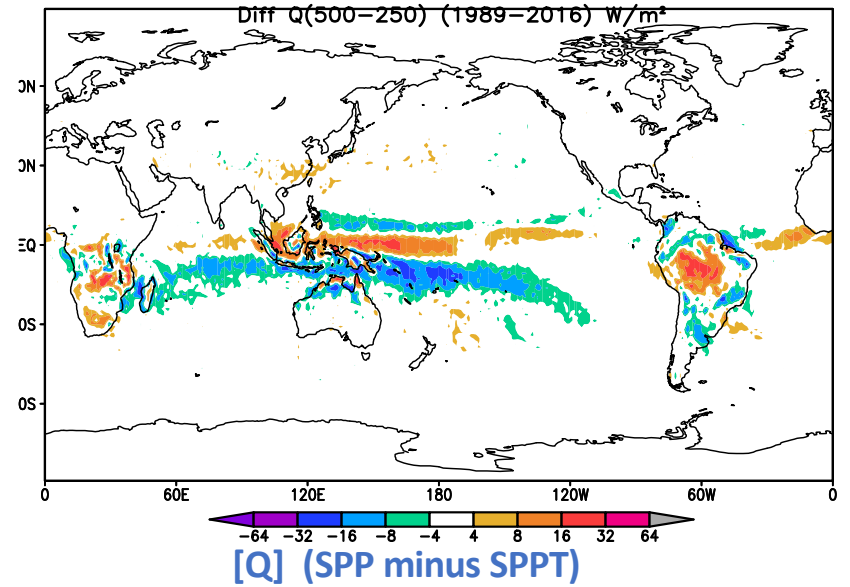
Mean differences of heating are *very small* – but with an interesting structure !

SPPT
Q (500-250
hPa)

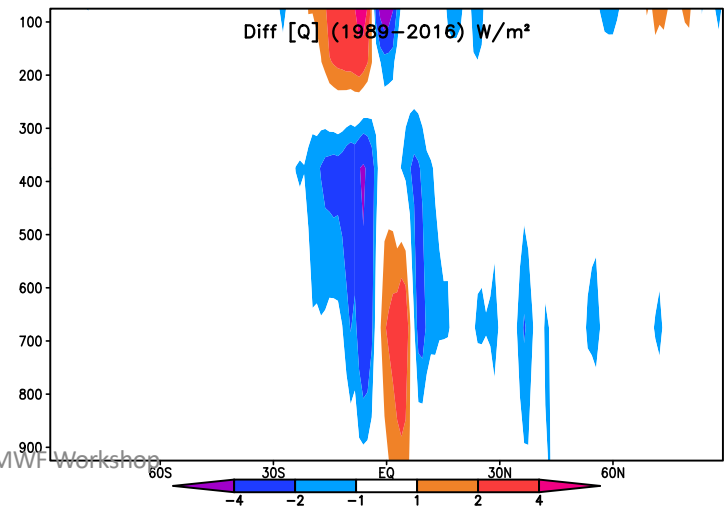
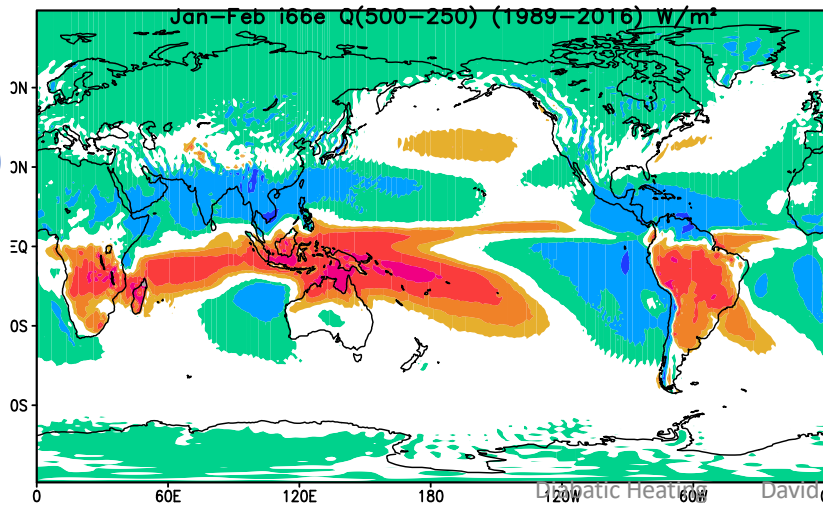
units:
 Wm^{-2}



Q (SPP minus SPPT) (500-250 hPa)



SPP
Q (500-250
hPa)



Comparison of Model Heating to “Observed” Heating or Apparent Heating Diagnosed from Reanalysis

“Observed” Heating techniques using satellite data typically diagnose latent heating based on:

(a) assumptions about the vertical structure of shallow vs. deep convection

or

(b) utilize a high-resolution limited area model (e.g. WRF) whose parameterizations make their own assumptions regarding the vertical structure of heating

Application of the residual technique (apparent heating) to reanalysis products.

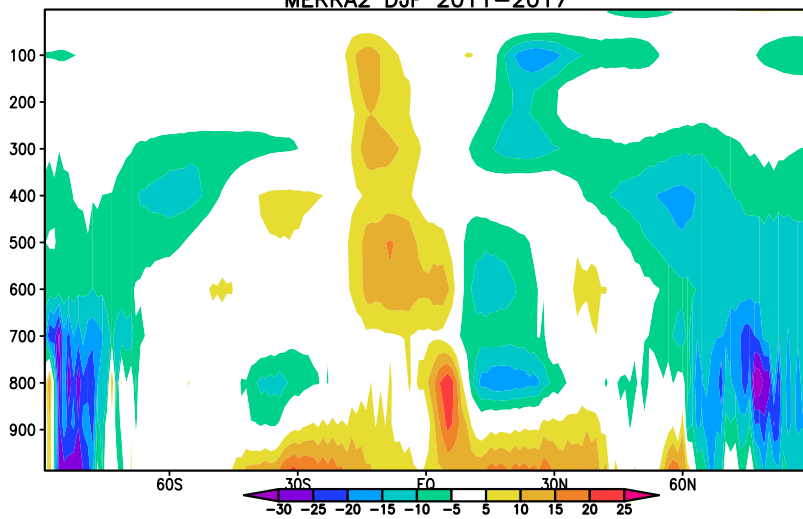
(a) Same technique can be used on all model output: Consistency of results

(b) BUT different reanalysis data sets used for verification don’t agree with each other in the upper troposphere and lower stratosphere

Apparently the difference in parameterizations in the forecast models used makes a difference in the analysis procedure, even in the presence of observations of the circulation and temperature

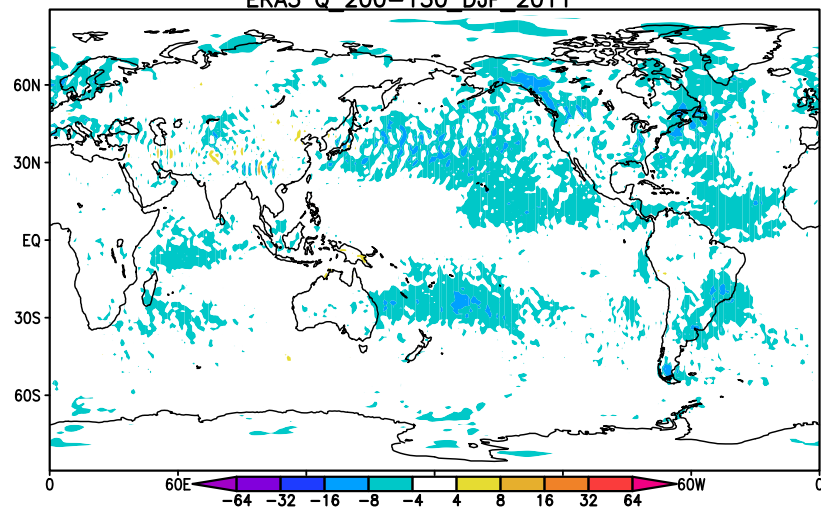
MERRA2 DJF 2011-2017

MERRA2
[Q]
Wm⁻²
DJF
2011-17



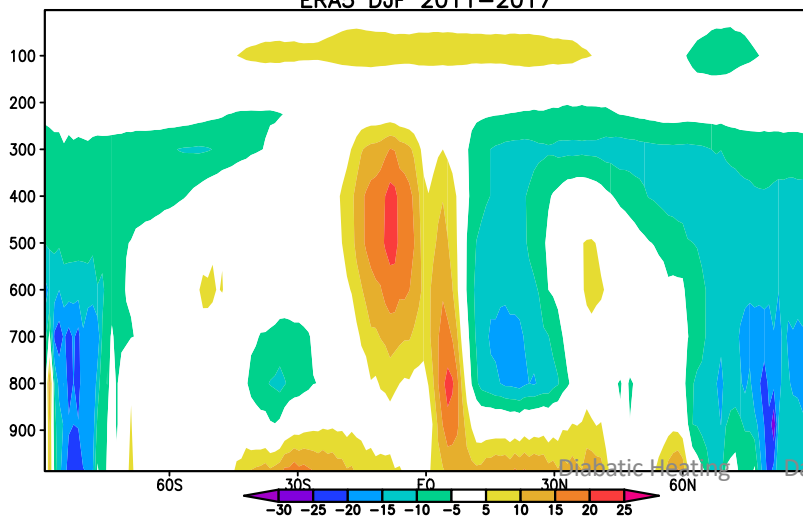
ERA5 Q 200-150 DJF 2011

ERA5
Q
200-150
DJF
2011-17



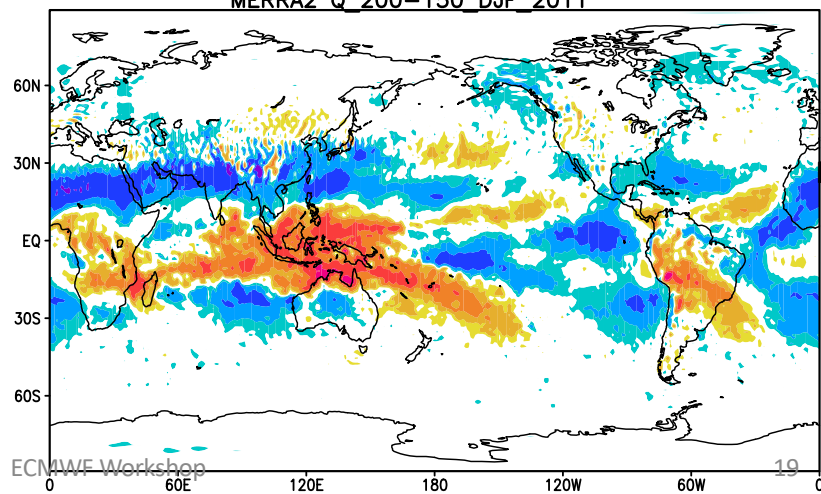
ERA5 DJF 2011-2017

ERA5
[Q]
Wm⁻²
DJF
2011-17



MERRA2 Q 200-150 DJF 2011

MERRA2
Q
200-150
DJF
2011-17



Some Brief Concluding Thoughts

- **Diabatic Heating is an important quantity to help understand the evolution of the atmosphere on weather to intra-seasonal to seasonal time scales**
- **The residual (“apparent heating”) method reasonably reproduces the true answer when we have it available from model forecasts/simulations**
- **There are still issues to be resolved regarding the heating diagnosed from reanalyses in the upper troposphere and lower stratosphere**

Appendix ("Apparent Heating" or Yanai Q1)

Use of thermodynamics in conjunction with the full 3-dimensional state of the atmosphere.

S is the entropy per unit mass, **Q** the rate of diabatic heating, thermodynamics tells us that:

$$T \frac{dS}{dt} = Q$$

where for an ideal gas the entropy is related to the potential temperature:

$$S = C_p \ln \Theta$$

$$\theta = T \left(\frac{p_0}{p} \right)^\kappa$$

$\kappa = R/C_p = 2/7$ where C_p is the specific heat per unit mass and R the gas constant

Taking $T \frac{ds}{dt} = Q$ and expressing the total (Lagrangian) derivative in Eulerian framework gives:

$$\frac{\partial \theta}{\partial t} + \vec{u} \cdot \vec{\nabla}(\theta) + \omega \frac{\partial \theta}{\partial p} = \frac{1}{C_p} \left(\frac{p_0}{p} \right)^\kappa Q$$

$$\frac{\partial \theta}{\partial t} + \vec{\nabla} \cdot (\vec{u}\theta) - \theta \vec{\nabla} \cdot (\vec{u}) + \omega \frac{\partial \theta}{\partial p} = \frac{1}{C_p} \left(\frac{p_0}{p} \right)^\kappa Q$$

$$C_p \left(\frac{p}{p_0} \right)^\kappa \left(\frac{\partial \theta}{\partial t} + \vec{\nabla} \cdot (\vec{u}\theta) - \theta D + \omega \frac{\partial \theta}{\partial p} \right) = Q$$

$\theta =$ potential temperature

$Q =$ rate of diabatic heating per unit mass

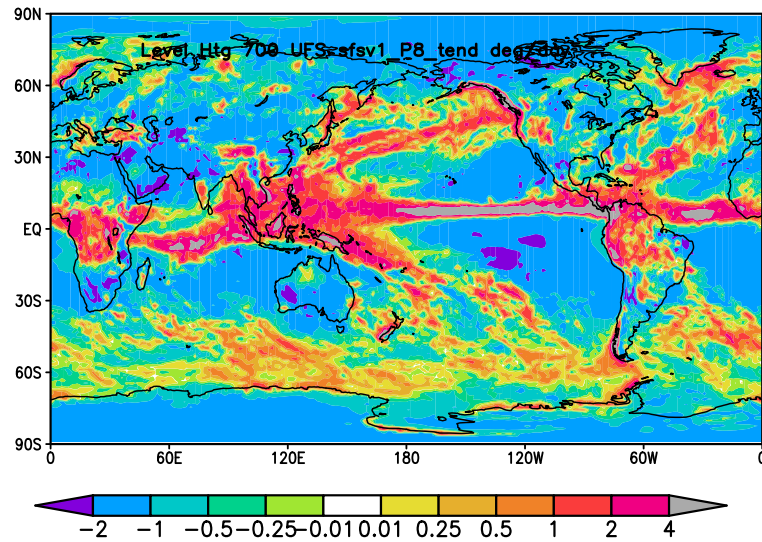
$\omega = \frac{dp}{dt} =$ vertical pressure velocity

$\vec{u} =$ horizontal wind vector = (u, v)

$\vec{u}_\theta = (u\theta, v\theta); D = \vec{\nabla} \cdot (\vec{u})$

$p =$ pressure ; $p_0 = 1000 \text{ hPa}; C_p = \frac{7}{2}R$

UFS P8 NOAA Model
Q taken **directly from model
parameterizations** for one
month (Oct 2011) in
deg/day



UFS P8 NOAA Model
Q **computed from the
thermodynamic equation**
for one month (Oct 2011) in
deg/day

